J Electr Eng Technol Vol. 9, No. 5: 1577-1581, 2014
http://dx.doi.org/10.5370/JEET.2014.9.5.1577

ISSN(Print) 1975-0102
ISSN(Online) 2093-7423

Minimization of Torque Ripple for an IPMSM with a Notched Rotor Using the Particle Swarm Optimization Method

Pan Seok Shin†, Ho Youn Kim* and Yong Bae Kim*

Abstract – This paper presents a method to minimize torque ripple of a V-type IPMSM using the PSO (Particle Swarm Optimization) method with FEM. The proposed algorithm includes one objective function and three design variables for a notch on the surface of a rotor. The simulation model of the V-type IPMSM has 3-phases, 8-poles and 48 slots with 2 notches on the one-pole rotor surface. The arc-angle, length and width of the notch are optimized to minimize the torque ripple of the motor. The cogging torque of the model is reduced by 55.6% and the torque ripple is decreased by 15.5 %. Also, the efficiency of the motor is increased by 15.5 %.

Keywords: Interior permanent magnet motor, Particle swarm optimization, Torque ripple, Notched rotor

1. Introduction

An Interior Permanent Magnet Synchronous Motor (IPMSM) has several advantages compared with a Surface Permanent Magnet Synchronous Motor (SPMSM). The IPMSM has a mechanically stable structure due to permanent magnets embedded in the rotor. It also has a slightly higher torque density per unit volume than other motors since the reluctance torque that results from an inductance difference between the d-axis and q-axis is combined with the magnetic torque. In addition, it is highly efficient and has a wide range of velocity control for low magnetic field operations. Thus, the IPMSM appears to be an excellent candidate for vehicle propulsion systems.

Unfortunately, the IPMSM produces significantly large torque ripple due to magnetic air gaps of similar length and mechanical structure. Therefore, the reduction of torque ripple that may cause vibration and acoustic noises becomes an increasingly critical issue in IPMSM. Currently, there are many studies on reducing such torque ripples, as well as cogging torque [1-3]. There are also a number of suggestions made on how to achieve this such as employing skew, adjusting of the number of slots per pole, controlling of the magnetizing region of the permanent magnet, and regulating the input current [4-5].

In this study, a 50 kW V-type IPMSM is modeled to reduce torque ripple by introducing two notches in the one-pole rotor surface as shown in Fig. 2. In the proposed algorithm, the position and size of the notch are optimized by an optimization algorithm, which uses a Latin Hypercube Sampling (LSH) strategy with a Response Surface Method (RSM) based on the multi-objective Pareto Optimization procedure. For obtaining an effective sampling point, PSO is also employed in the algorithm. To verify the proposed method, the simulation model is applied to and analyzed by the FE program [6-7].

† Corresponding Author: Dept. of Electronic Engineering, Hongik Univerity, Sejong City 339-701, Korea. (psshin@hongik.ac.kr)
* Dept. of Electronic Engineering, Hongik Univerity, Sejong City 339-701, Korea. ({hoyoun100, nhb0108}@ naver.com)
Received: February 20, 2013; Accepted: April 1, 2014

2. Simulation Model and Specifications

Table 1 describes the main specifications of the simulation model of the IPMSM. The capacity of the motor is 50 kW with a speed of 1200~1500 rpm, a rated voltage of 500 V, 3 phases, 8 poles and 48 slots. The current has a wide range according to its operational conditions. In the FE simulation, 200 A is used as the rated current. Fig. 1 shows a cross-section of the simulation model (one pole) and the FE meshes. The total number of meshes is approximately 7,400. A double-layer mesh is used in an air gap to calculate the force and torque of the model using a rotating air gap and external circuit. Fig. 2 shows the optimization model of the notch, which has two design variables (i.e., notch angular length, l_n, and pitch angle between notches, θ_N) and one constraint. The notch angular length, l_n, is constraint between 0.5 and 3[°], the pitch angle between notches, θ_N, is constraint between 8 and 20 [°] while the notch depth, d_n, is kept at 0.5[mm]. Fig. 2(a) shows an FEM model of the motor (one pole) while Fig. 2(b) shows the FE meshes.

Table 1. Specifications of the 50 kW IPMSM model

Capacity [kW]	50	No. of Poles	8
Rated speed[rpm]	1200	No. of Phases	3
Max. speed[rpm]	6000	No. of Slots	48
Rated voltage[V]	500	Magnet	NdFeB
Current[A]	≤200	Frequency[Hz]	80

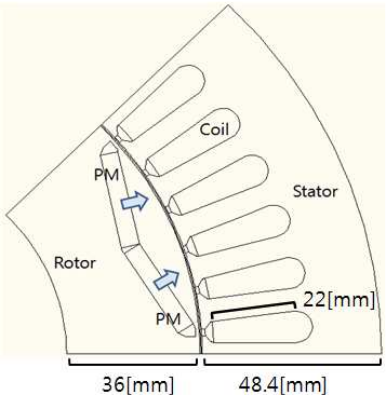

(a) FEM model of BLDC motor

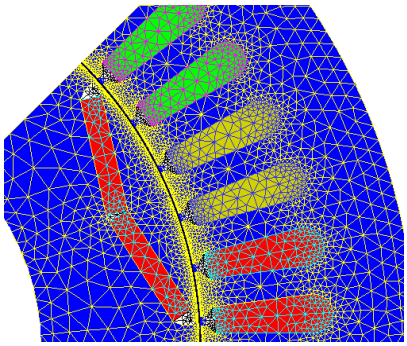

(b) FE Meshes of the model

Fig. 1. Simulation model of a V-type IPMSM (one pole) with FE meshes

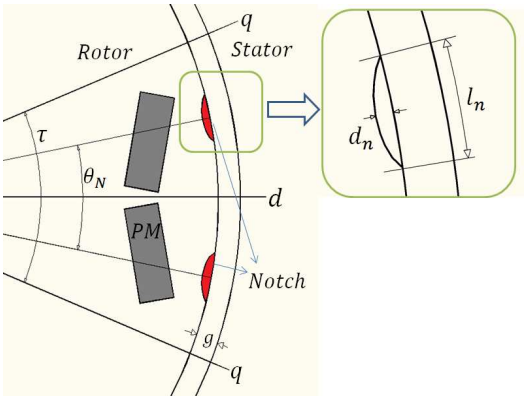

Fig. 2. Notch model of a rotor's surface for a V-type IPMSM

Fig. 3(a) shows the flux density distribution of the optimized model around the PM and the notch. Fig. 3(b) shows the flux density profiles along the center line of the air gap with/without the notch on the rotor's surface. The horizontal axis of Fig. 3(b) is 'Rotor position'; that is one pole of PM(0 to 180 degree). In the case of the notch, the average flux density is slightly lower than for the case of a rounded surface, as expected.

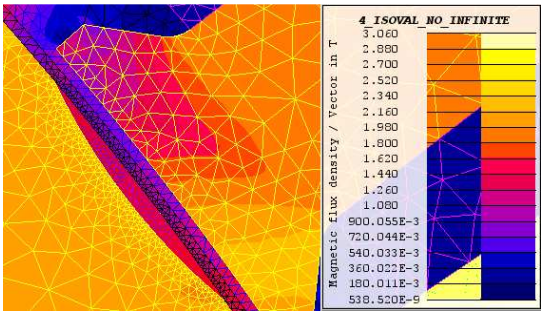

(a) Flux density around the notch

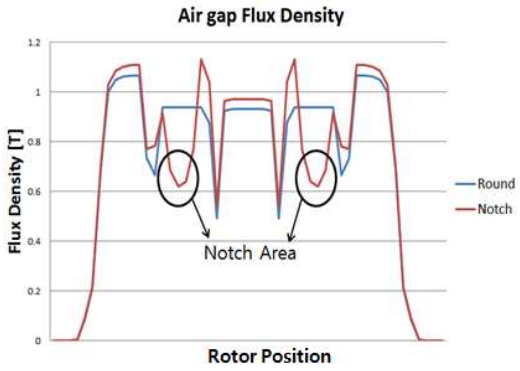

(b) Flux density profiles in air gap

Fig. 3. (a) Flux density distribution around the notch; (b) Flux density profiles along the center line of the air gap (the average flux density is 0.703[T])

3. Optimization Algorithm with PSO

3.1 Cogging torque calculation

Torque perturbations arise from the variations of magnetic energy associated to a change in airgap length, as the rotor rotates without load current. Since the energy change in a PM and iron is negligible compared to that of air, the magnetostatic energy is given as [5],

$$W(a) \cong W(a)_{airgap} = \frac{1}{2\mu_0}\int [P(\theta) \cdot F_m(\theta, a)]^2 dV \,, \qquad (1)$$

Where μ_0, $P(\theta)$ and $F_m(\theta, a)$ represent the permeability of air, the air gap permeance function, and the air gap MMF function, respectively. The cogging torque for a PM brushless motor can be expressed as

$$\begin{aligned} T(a) &= -\frac{\partial W(a)_{airgap}}{\partial a} \\ &= \frac{L_s \pi}{4\mu_0}(R_s^2 - R_m^2) \cdot \sum_{n=0}^{\infty} nN_L G_{nN_L} B_{nN_L} \sin nN_L a \end{aligned} \qquad (2)$$

where L_s, R_s, R_m and G_{nN_L}, B_{nN_L} denote the stack length, the stator bore radius, the magnet outer radius, and

the corresponding Fourier coefficients of the relative air gap permeance and the flux density function, respectively [5]. Eq. (2) reveals that the cogging torque is first governed by N_L, G_{nNL} and B_{nN_L} with the fundamental period of $2\pi/N_L$, where N_L is the least common multiple of number of stator and rotor poles.

3.2. LHS and RMS

Latin Hypercube Sampling is a "space filling" experimental design strategy [6]. The RSM with a multi-quadric radial basis function is widely used for global interpolations. It is also very efficient due to its smoothness and fitting ability when given a limited number of sampling points. As such,

$$S(x) = \sum_{i=1}^{N} c_i g(x - x_i),\ g(x) = \sqrt{|x|^2 + r^2} \tag{3}$$

where x is the design parameter vector, c_i is the coefficient corresponding to the i-th sampling point x_i, g(x) is the multi-quadric radial basis function, and r is so called "shape parameter" whose purpose is to control the curvature of the single basis function near the center point [7-8].

3.3. PSO (Particle Swarm Optimization Method)

Particle Swarm Optimization is a heuristic search technique that simulates the movements of a flock of birds which aim to find food. This method is advantageous in terms of relative simplicity, quick convergence requiring less computing, and effective locating of all local optimum points. These points in turn are motivated by the clustering PSO algorithm [9-10].

Fig. 4 shows the procedure of the proposed optimization program with PSO. The PSO algorithm has five steps to determine an optimal sampling point: 1) identify main particle movements, 2) locate main particles that form a couple, 3) isolate a non-stop couple, 4) eliminate near-by couples, and 5) assess movement stopping criterion. The algorithm ends when the iteration number is reached at a pre-set figure, when an optimized position is found, or when the criteria of the objective function satisfy a pre-defined value.

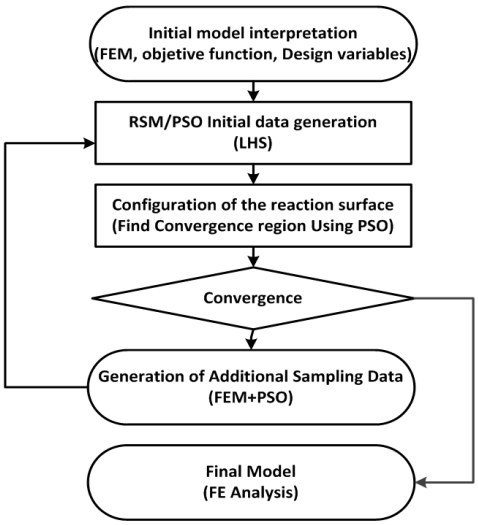

Fig. 4. Flow chart of PSO based optimization algorithm

4. Simulation and Results

Two design variables, l_n, θ_N, of the notch are constrained as shown in Fig. 4. Using the proposed optimization algorithm with PSO, 125 sampling points are selected through 5 iterations. The objective function to minimize the torque ripple is described as Eq. (4).

$$Minimize\ F_{obj} = \sum_{i} \left(\frac{\tau_{i+1} - \tau_i}{\tau_{i+1}} \right)^2 \tag{4}$$

where τ_{i+1} is the torque ripple at (i+1)-th iteration and τ_i is the average torque at i-th iteration. Fig. 5 shows three cases of the notch shape at a different length and arc angle; Fig. 5(a) θ_N=20[°], Fig. 5(b) θ_N=8[°] and Fig. 5(c) at θ_N=14.75[°]. As observed, Fig. 5(c) is the optimized model. Table 2 describes the optimized notch length, l_n, the arc angle of θ_N and the torque ripple at each step of the optimization program. It should be noted that as the step increases, the torque ripple converges to 96.3 N.m. Fig. 6 shows the average torque ripple of the optimized model as a function of the iteration steps. After the 5th iteration step, the optimized arc angle, θ_N, is 14.74[°] and the notch angle, l_n, is 2.38[°].

As shown in Fig. 7, the optimized cogging torque is

Table 2. Optimized variable and torque ripple at each step

Step	θ_N [°]	l_n [°]	Torque ripple [N.m]
1st	15.51	1.65	96.72
2nd	14.54	3.00	96.57
3rd	14.66	2.78	96.30
4th	14.75	2.38	96.28
5th	14.74	2.38	96.284

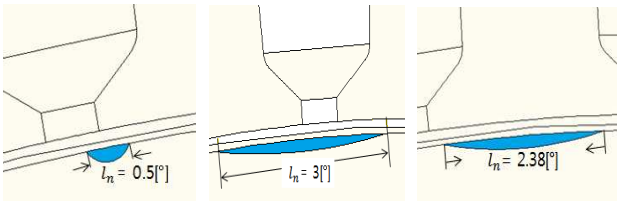

(a) θ_N=20[°] (b) θ_N=8[°] (c) θ_N=14.75[°]

Fig. 5. Simulation model of the notch on the rotor's surface

reduced by 56.4% from 7.30 [N.m] to 3.19 [N.m]. Also, the torque ripple is reduced by 4.41 % as seen in Fig. 8. With the notch, the optimized T_{max} is 437.6[N. m], T_{min} is 340.8 [N.m], and T_{avg} is 389.1 [N.m]. However, without the notch (i.e., for a rounded surface), T_{max} is 448.9 [N.m],

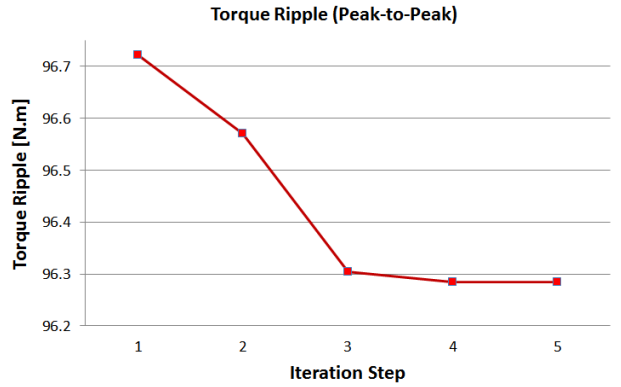

Fig. 6. Average torque ripple of the optimized model as a function of the iteration steps

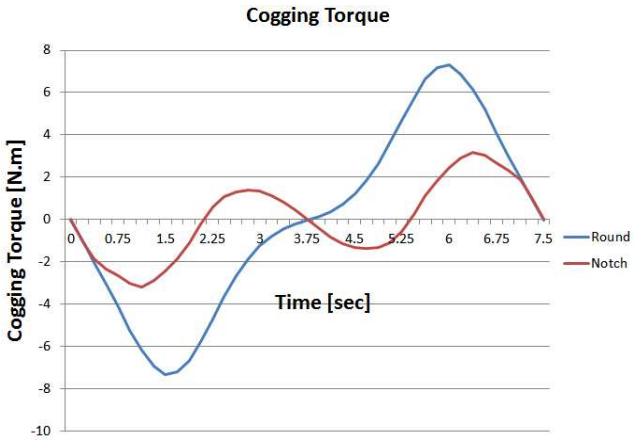

Fig. 7. Comparison of cogging torque between the round and the notched surface model(The final value of θ_N =14.74[°] and l_n =2.38 [°])

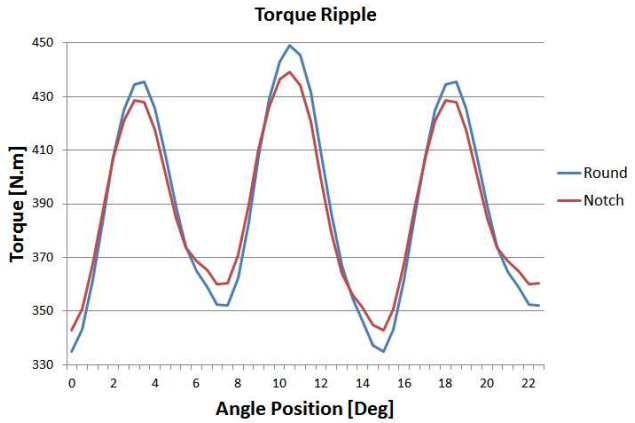

Fig. 8. Comparison of torque profiles between the round and the notched surface model model(The final value of θ_N =14.74[°] and l_n =2.38 [°])

T_{min} is 335.1 [N.m], and T_{avg} is 389.2 [N.m].

The torque ripple ratio can be calculated as in Eq. (5),

$$T_{rr} = \left(\frac{T_{max} - T_{min}}{T_{avg}} \right) \times 100 \qquad ()$$

where T_{rr} , T_{max} , T_{min} , T_{avg} denote the torque ripple ratio, the maximal torque, the minimal torque, and the average torque, respectively.

5. Conclusions

In this study, an optimization algorithm is proposed to minimize the torque ripple of a V-type IPMSM using a particle swarm optimization method with FEM. In the algorithm, an LHS strategy is incorporated with RSM based on a multi-objective Pareto Optimization procedure. PSO is also used to obtain an effective sampling point.

In order to verify the effectiveness of the proposed algorithm, the notch shape on the rotor's surface of a 50 kW IPMSM is optimally formed with 2 design parameters and several constraints for minimizing torque ripple. The simulation model of the V-type IPMSM has 3-phases, 8-poles and 48 slots with 2 notches on the one-pole rotor surface. The arc-angle, length and width of the notch are optimized to minimize the torque ripple of the motor. In so doing, the cogging torque of the optimized model is thus reduced by 56.4% and the torque ripple is decreased by 4.41 %. In addition, the efficiency of the motor is increased by 15.5 %.

Acknowledgment

This research was supported by Basic Science Research Program through the National Research Foundation of Korea(NRF) funded by the Ministry of Education (2012R1A1A4A01010937), and partially by the International Science and Business Belt Program through the Ministry of Science, ICT and Future Planning (2013K000468)

References

[1] A. Kisoumarsi, M. Moalle, and B. Fashimi, "Midigation of Torque Ripple in Interior Permanent Magnet Motors by Optical Shape Design", *IEEE Transactions on Magnetics,* vol. 42, no. 11, pp. 3706-3711, Nov.2005.

[2] G.-H. Kang, J.-P. Hong, G.-T. Kim, and J.-W. Park, "Improved parameter modeling of interior permanent magnet synchronous motor based on finite element analysis," *IEEE Transactions on Magnetics,* vol. 36,

no. 4, pp. 1867-1870, Jul. 2000.

[3] S.H. Thomas, T.M. Jahns, and W.L. Soong, "Torque Ripple Reduction in Interior Permanent Magnet Synchronous Machines Using the Principle of Mutual Harmonics Exclusion," Industry Applications Conference, 2007. 42nd IAS Annual Meeting. Conference Record of the 2007 IEEE, vol. no. pp. 558-565.

[4] J. R. Hendershot Jr., TJE Miller "Design of Brushless Permanent-Magnet Motors", Magna Physics Publishing and Clarendon Press, Oxford, 1994.

[5] S. M. Hwang, J. B. Eom, G. B. Hwang, W. B. Jeong, Y. H. Jung, "Cogging Torque and Acoustic Noise Reduction in Permanent Magnet Motor by Teeth Pairing", *IEEE Trans. on Magnetics,* vol. 36, pp. 3144-3146, September 2000.

[6] Yanli Zhang, H.S. Yoon and C.S. Koh, "Study on a Robust Optimization Algorithm Using Latin Hypercube Sampling Experiment and Multiquadric Radial Basis Function", *Proceeding of KIEE EMECS Annual Spring Conference*, pp.162-164, April 2007.

[7] P. S. Shin, et.al., "Shape Optimization of a Large-Scale BLDC Motor Using an Adaptive RSM Utilizing Design Sensitivity Analysis," *IEEE Trans. on Magnetics*, vol. 43, no. 4, pp. 1653-1656, April 2007.

[8] P.S. Shin, S.H. Woo, C.S. Koh, "An Optimal Design of Large Scale Permanent Magnet Pole Shape Using Adaptive Response Surface Method With Latin Hypercube Sampling Strategy", *Io--------0-0pEEE Transactions on Magnetics*, vol. 45, no. 3, pp. 1214-1217, March 2009.

[9] James Kennedy and Russell Eberhart. "Particle Swarm Optimization."

[10] *In proceedings of the IEEE International Conference on Neural Networks*, volume 4, pp. 1942-1948, Piscataway, NJ 1995, IEEE.

[11] Y. B. Kim, Hong Soon Choi, C. S. Koh and P. S. Shin "A Back EMF Optimization Double Layered Large Scale BLDC Motor by Using Hybrid Optimization Method", *IEEE Transactions on Magnetics*, vol. 45, no. 5, pp. 998-1001, May 2011.

Yong Bae Kim He received B.S and M.S. degrees in electrical engineering from Hongik University, 2009 and 2011. He is a Ph.D student in Department of Electrical Engineering of Hongik University.

Ho Youn Kim He received B.S and M.S. degrees in electrical engineering from Hongik University, 2011 and 2013. He works at Keyang Electric Company as a researcher.

Pan Seok Shin He received B.S. in electrical engineering from Seoul National University, and received Ph.D in electric power engineering from Rensselaer Polytechnic Institute in 1989. He works at Hongik University as a professor since 1993.